Local forest structure variability increases resilience to wildfire in dry western U.S. coniferous forests

Michael J. Koontz[1,2,3*], Malcolm P. North[2,4], Chhaya M. Werner[2,5,6], Stephen E. Fick[7,8], Andrew M. Latimer[2]

[1]Graduate Group in Ecology, University of California; Davis, CA, USA

[2]Department of Plant Sciences, University of California; Davis, CA, USA

[3]Earth Lab, University of Colorado-Boulder; Boulder, CO, USA

[4]Pacific Southwest Research Station, USDA Forest Service; Mammoth Lakes, CA, USA

[5]Center for Population Biology, University of California; Davis, CA, USA

[6]German Centre for Integrative Biodiversity Research; Halle-Jena-Leipzig, Germany

[7]US Geological Survey, Southwest Biological Science Center

[8]Department of Ecology and Evolutionary Biology, University of Colorado; Boulder, CO, USA

[*]*Correspondence:* 4001 Discovery Drive; Boulder, CO 80303; michael.koontz@colorado.edu; (970) 682-4727

Coauthor emails: mnorth@ucdavis.edu (MPN), cwerner@ucdavis.edu (CMW), stephen.fick@gmail.com (SEF), amlatimer@ucdavis.edu (AML)

Running title: Remote sensing resistance

Keywords: resilience, wildfire, severity, texture analysis, forest structure, Sierra Nevada, forest, disturbance

Type of article: Letters

Abstract word count: 149

Main text word count: 5435 (Intro: 1184; Methods: 1829 (891 + 692 + 246); Results: 550 (179 + 371); Discussion: 1872)

Text boxes word count: 0

Number of... references: 106, figures: 5, tables: 1, text boxes: 0

Statement of authorship: MJK, CMW, SEF, MPN, and AML conceived the study. MJK, SEF, and CMW wrote the Earth Engine code. MJK performed the analysis, with input from all authors. MJK wrote the first draft of the manuscript. All authors contributed substantially to editing and revisions.

Data accessibility statement: The data and analysis code supporting the results are archived on the Open Science Framework at www.doi.org/10.17605/OSF.IO/27NSR.

Date report generated: October 20, 2019

Abstract

A "resilient" forest endures disturbance and is likely to persist. Resilience to wildfire may arise from feedback between fire behavior and forest structure in dry forest systems. Frequent fire creates fine-scale variability in forest structure, which may then interrupt fuel continuity and prevent future fires from killing overstory trees. Testing the generality and scale of this phenomenon is challenging for vast, long-lived forest ecosystems. We quantify forest structural variability and fire severity across >30 years and nearly 1,000 wildfires in California's Sierra Nevada. We find that greater variability in forest structure increases resilience by reducing rates of fire-induced tree mortality and that the scale of this effect is local, manifesting at the smallest spatial extent of forest structure tested (90m x 90m). Resilience of these forests is likely compromised by structural homogenization from a century of fire suppression, but could be restored with management that increases forest structural variability.

Introduction

Forests are essential components of the biosphere, and ensuring their persistence is of high management priority given their large carbon stores and other valued ecosystem services (Hansen *et al.* 2013; Crowther *et al.* 2015; Millar & Stephenson 2015; Trumbore *et al.* 2015; Higuera *et al.* 2019). Modern forests are subject to disturbances that are increasingly frequent, intense, and entangled with human society, which may compromise their resilience and their ability to persist (Millar & Stephenson 2015; Seidl *et al.* 2016; Schoennagel *et al.* 2017; Hessburg *et al.* 2019; McWethy *et al.* 2019). A resilient forest can absorb disturbances and may reorganize, but is unlikely to transition to an alternate vegetation type in the long run (Holling 1973; Walker *et al.* 2004; Scheffer 2009; Reyer *et al.* 2015a). Resilience can arise when interactions amongst heterogeneous elements within a system create stabilizing negative feedbacks, or interrupt positive feedbacks that would otherwise cause critical transitions (Peters *et al.* 2004; Reyer *et al.* 2015a). System resilience can be generated by heterogeneity at a variety of organizational scales, including genetic diversity (Reusch *et al.* 2005; Agashe 2009; Baskett *et al.* 2009), species diversity (Tilman 1994; Chesson 2000; Cadotte *et al.* 2013), functional diversity (Gazol & Camarero 2016), topoclimatic complexity (Ackerly *et al.* 2010; Lenoir *et al.* 2013), and temporal environmental variation (Questad & Foster 2008). Forest resilience mechanisms are fundamentally difficult to quantify because forests comprise long-lived species, span large geographic extents, and are affected by disturbances at a broad range of spatial scales (Reyer *et al.* 2015a, b). It is therefore critical, but challenging, to understand the system-wide mechanisms underlying forest resilience and the extent to which humans have the capacity to influence them.

Wildfire severity describes a fire's effect on vegetation (Keeley 2009) and high-severity fire, in which all or nearly all overstory vegetation is killed, can be a precursor to state transitions in dry coniferous forests (Stevens *et al.* 2017; Davis *et al.* 2019). For several centuries prior to Euroamerican invasion, fire regimes in this ecosystem were variable as a consequence of both natural and Indigenous burning, with primarily low- and moderate-severity fire and localized patches of high-severity fire (Safford & Stevens 2017). Most dry coniferous tree species in frequent-fire forests did not evolve mechanisms to protect propagules (e.g., seeds, buds/stems that can resprout) through high-severity fire, so recruitment in large patches with few or no surviving trees is often highly limited by longer-distance dispersal of tree seeds from unburned or lower-severity areas (Welch *et al.* 2016; Stevens *et al.* 2017; Young *et al.* 2019). In the Sierra Nevada, the absence of tree seeds after severe wildfire can lead to forest regeneration failure as resprouting shrubs outcompete slower-growing conifer seedlings and provide continuous cover of flammable fuel that makes future high-severity wildfire more likely (Collins & Roller 2013; Coppoletta *et al.* 2016), though this pathway doesn't materialize in forests with a slower post-fire vegetation response such as those in the Pacific Northwest (Prichard & Kennedy 2014; Stevens-Rumann *et al.* 2016). Dry forest regeneration is especially imperiled after high-severity fire when post-fire climate conditions are suboptimal for conifer seedling establishment (Davis *et al.* 2019) or optimal for shrub regeneration (Young *et al.* 2019).

Many dry western U.S. forests are experiencing "unhealthy" conditions which leaves them prone to catastrophic shifts in ecosystem type (Millar & Stephenson 2015; McWethy *et al.* 2019). First, a century of fire suppression has drastically increased forest density and fuel connectivity (Safford & Stevens 2017), which increases competition for water (D'Amato *et al.* 2013; van Mantgem *et al.* 2016) and favors modern wildfires with large, contiguous patches of tree mortality whose interiors are far from potential seed sources (Miller & Thode 2007; Safford & Stevens 2017; Stevens *et al.* 2017; Steel *et al.* 2018). Second, warmer temperatures coupled with recurrent drought (i.e., "hotter droughts") exacerbate water stress on trees (Williams *et al.* 2013; Millar & Stephenson 2015; Clark *et al.* 2016), producing conditions favorable for high-intensity fire (Fried *et al.* 2004; Abatzoglou & Williams 2016) and less suitable for post-fire conifer establishment (Stevens-Rumann *et al.* 2018; Davis *et al.* 2019). Thus, the presence of stabilizing feedbacks that limit high-severity fire may represent a fundamental resilience mechanism of dry coniferous forests, but anthropogenic climate and management impacts may be upsetting those feedbacks and eroding forest resilience.

An emerging paradigm in forest ecology is that resilience to disturbances such as wildfire may derive from heterogeneity in vegetation structure (Turner & Romme 1994; Stephens *et al.* 2008; North *et al.* 2009; Virah-Sawmy *et al.* 2009). Forest structure– the size and spatial distribution of vegetation in a forest– links past and future fire disturbance via feedbacks with fire behavior (Agee 1996). A structurally variable

forest with horizontally and vertically discontinuous fuel may experience slower-moving surface fires, a lower probability of crown fire initiation and spread, and a reduced potential for self-propagating, eruptive behavior (Scott & Reinhardt 2001; Graham *et al.* 2004; Peters *et al.* 2004; Stephens *et al.* 2009; Fox & Whitesides 2015; Parsons *et al.* 2017). Feeding back to influence forest structure, this milder fire behavior, characteristic of pre-Euroamerican settlement conditions in dry western U.S. forests, generates a heterogeneous patchwork of fire effects including consumed understory vegetation, occasional overstory tree mortality, and highly variable structure at a fine scale (Sugihara *et al.* 2006; Scholl & Taylor 2010; Cansler & McKenzie 2014; Safford & Stevens 2017). Thus, more structurally variable dry forests are often considered more resilient and are predicted to persist in the face of frequent wildfire disturbance (Graham *et al.* 2004; Moritz *et al.* 2005; Stephens *et al.* 2008).

While the homogenizing effect of modern high-severity fire on forest structure is well-documented (Steel *et al.* 2018), the foundational concept of feedback between heterogeneity of forest structure and fire severity is underexplored at the ecosystem scale, in part because of the dual challenges of measuring fine-grain vegetation heterogeneity at broad spatial extents (Kane *et al.* 2015; Graham *et al.* 2019) and linking local, bottom-up processes to emergent ecosystem-wide patterns in an empirical setting (Turner & Romme 1994; Bessie & Johnson 1995; McKenzie & Kennedy 2011, 2012). Furthermore, it has been difficult to resolve the "scale of effect" (*sensu* Graham *et al.* 2019) for how variability in forest structure is meaningful for resilience (Kotliar & Wiens 1990; Turner *et al.* 2013).

Recent advances in the accessibility and tractability of spatiotemporally extensive Earth observation data (Gorelick *et al.* 2017) provide an avenue to insight into fundamental ecosystem properties at relevant scales, such as resilience mechanisms of vast, long-lived forests. We use Landsat satellite imagery and a massively-parallel image processing approach to calculate wildfire severity for over 1,000 Sierra Nevada yellow pine/mixed-conifer wildfires encompassing a wide size range (4 to >100,000 hectares) and long time series (1984 to 2018). We calibrate these spectral severity measures to ground assessments of fire effects on overstory trees from over 200 field plots. For each point within these ~1,000 fires, we use texture analysis (Haralick *et al.* 1973) at multiple scales in order to characterize local variability in vegetation structure across broad spatial extents and determine its "scale of effect" (Graham *et al.* 2019). We pair the resulting extensive database of wildfire severity and multiple scales of local forest variability to ask: (1) Does spatial variability in forest structure increase the resilience of California yellow pine/mixed-conifer forests by reducing the severity of wildfires? (2) What is the "scale of effect" of structural variability that influences wildfire severity? and (3) Does the influence of structural variability on fire severity depend on topography, regional climate, or other conditions?

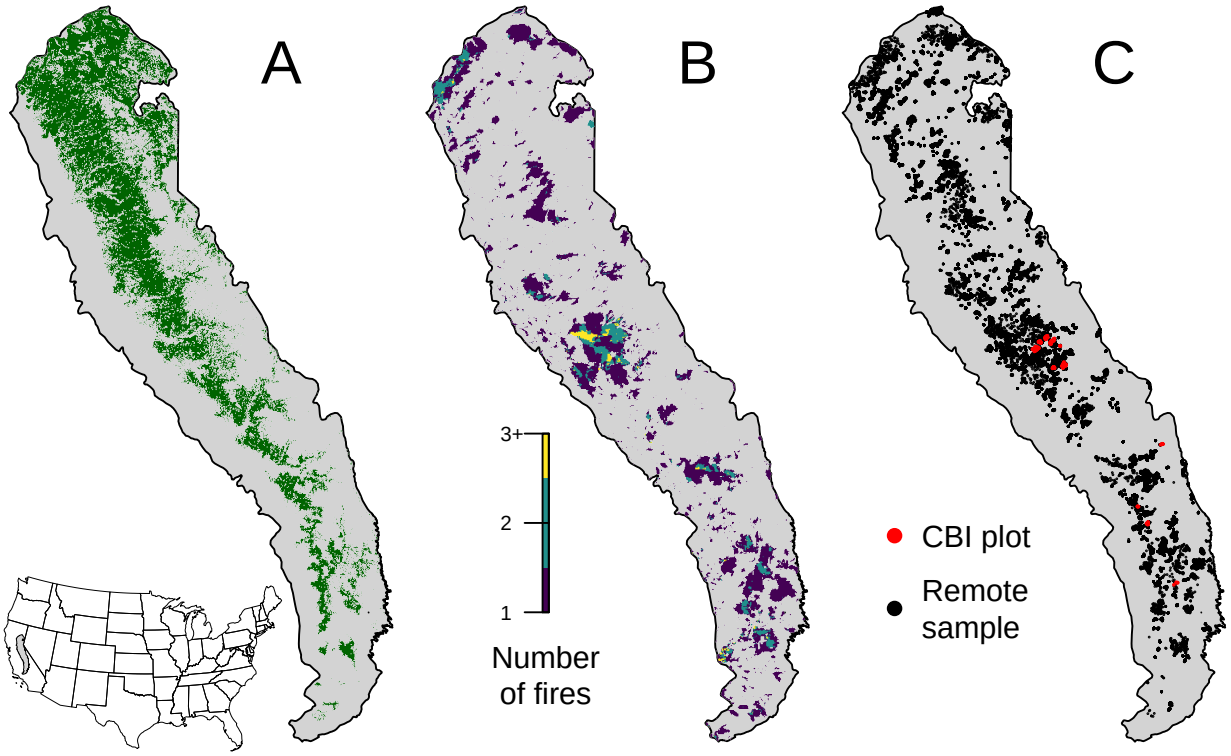

Fig. 1. Geographic setting of the study. A) Location of yellow pine/mixed-conifer forests as designated by the Fire Return Interval Departure (FRID) product which, among other things, describes the potential vegetation in an area based on the pre-Euroamerican settlement fire regime. B) Locations of all fires covering greater than 4 hectares that burned in yellow pine/mixed-conifer forest between 1984 and 2018 in the Sierra Nevada mountain range of California according to the State of California Fire Resource and Assessment Program database, the most comprehensive database of fire perimeters of its kind. Colors indicate how many fire perimeters overlapped a given pixel within the study time period. C) (red) Locations of 208 composite burn index (CBI) ground plots used to calibrate the remotely sensed measures of severity. (black) Locations of random samples drawn from 1008 unique fires depicted in panel B that were in yellow pine/mixed-conifer forest as depicted in panel A, and which were designated as "burned" by exceeding a threshold relative burn ratio (RBR) determined by calibrating the algorithm presented in this study with ground-based CBI measurements.

Material and Methods

Study system

Our study assesses the effect of vegetation structure on wildfire severity in the Sierra Nevada mountain range of California in yellow pine/mixed-conifer forests (Fig. 1). This system is dominated by a mixture of conifer species including ponderosa pine (*Pinus ponderosa*), sugar pine (*Pinus lambertiana*), incense-cedar (*Calocedrus decurrens*), Douglas-fir (*Pseudotsuga menziesii*), white fir (*Abies concolor*), and red fir (*Abies magnifica*), angiosperm trees primarily including black oak (*Quercus kelloggii*), as well as shrubs (*Ceanothus* spp., *Arctostaphylos* spp.) (Safford & Stevens 2017). We considered "yellow pine/mixed-conifer forest"

to be all areas designated as a yellow pine, dry mixed-conifer, or moist mixed-conifer pre-settlement fire regime (PFR) in the USFS Fire Return Interval Departure database (https://www.fs.usda.gov/detail/r5/landmanagement/gis/?cid=STELPRDB5327836), which reflects potential vegetation and is less sensitive to recent land cover change (Steel *et al.* 2018). We considered the Sierra Nevada region to be the area within the Sierra Nevada Foothills, the High Sierra Nevada, and the Tehachapi Mountain Area Jepson ecoregions (JepsonFloraProject 2016).

A programmatic remote sensing assessment of wildfire severity

We measured forest vegetation characteristics and wildfire severity using imagery from the Landsat series of satellites (Eidenshink *et al.* 2007; Miller & Thode 2007) post-processed to surface reflectance using radiometric corrections (Masek *et al.* 2006; Vermote *et al.* 2016; USGS 2017b, a). Landsat satellites image the entire Earth approximately every 16 days with a 30m pixel resolution. We used Google Earth Engine, a massively parallel cloud-based geographic information system and image hosting platform, for all image collation and processing (Gorelick *et al.* 2017).

We calculated wildfire severity for the most comprehensive digital record of fire perimeters in California: The California Department of Forestry and Fire Protection, Fire and Resource Assessment Program (FRAP) fire perimeter database (https://frap.fire.ca.gov/frap-projects/fire-perimeters/). Smaller fire events are important contributors to fire regimes, but their effects are often underrepresented in analyses of fire effects (Randerson *et al.* 2012). The FRAP database includes all known fires that covered more than 4 hectares, compared to the regional standard database which includes fires covering greater than 80 hectares (Miller & Thode 2007; Miller & Safford 2012; Miller *et al.* 2012; Steel *et al.* 2018) and the national standard Monitoring Trends in Burn Severity (MTBS) database which includes fires covering greater than 400 hectares in the western U.S. (Eidenshink *et al.* 2007). The FRAP perimeters go through substantial error checking, but it is possible that duplicated events are occasionally represented in the database. Using the FRAP database of fire perimeters, we quantified fire severity within each perimeter of 1008 wildfires in the Sierra Nevada yellow pine/mixed-conifer forest that burned between 1984 and 2018, which more than doubles the number of fire events represented from 432 to 1008 compared to the regional standard database.

We created per-pixel median composites of collections of pre- and postfire images for each fire to calculate common spectral indices of wildfire severity. Prefire image collections spanned a fixed time window ending one day before the fire's discovery date and postfire image collections spanned the same fixed time window, exactly one year after the prefire window. We tested four different time periods (16, 32, 48, and 64 days) that defined the time window of the pre- and postfire image collections, and seven common spectral indices of

severity (RBR, dNBR, RdNBR, dNBR2, RdNBR2, dNDVI, RdNDVI) for a total of 28 different means to remotely measure wildfire severity. See supplemental methods for full details of spectral measures of wildfire severity.

We calibrated these 28 severity metrics with 208 field measures of fire effects to overstory vegetation—measured as the overstory component of the Composite Burn Index (CBI)— from two previously published studies (Zhu *et al.* 2006; Sikkink *et al.* 2013). CBI is a metric of vegetation mortality across several vertical vegetation strata within a 30m diameter field plot, and the overstory component characterizes fire effects to the overstory vegetation specifically, which includes both dominant/co-dominant big trees as well as intermediate-sized subcanopy trees (generally 10-25 cm DBH and 8-20m tall) (Key & Benson 2006). CBI ranges from 0 (no fire impacts) to 3 (very high fire impacts), and has been successfully used as a standard for calibrating remotely-sensed severity data in western U.S. forests (Key & Benson 2006; Miller & Thode 2007; Miller *et al.* 2009; Cansler & McKenzie 2012; Parks *et al.* 2014, 2018a; Prichard & Kennedy 2014). We interpolated each remotely-sensed severity metric using both bilinear (mean of 4 nearest pixels) and bicubic interpolation (mean of 16 nearest pixels) (Cansler & McKenzie 2012; Parks *et al.* 2014, 2018a) and fit a non-linear model following Miller & Thode (2007), Miller *et al.* (2009), Parks *et al.* (2014), and Parks *et al.* (2018a) to each remotely-sensed severity metric of the following form:

(1) $\text{remote\_severity} = \beta_0 + \beta_1 e^{\beta_2 \text{cbi\_overstory}}$

We treated the remotely-sensed severity measure as the dependent variable for comparison with other studies linking spectral severity with CBI (Miller & Thode 2007; Parks *et al.* 2014). We performed ten-fold cross validation using the `modelr` and `purrr` packages in R (R Core Team 2018; Henry & Wickham 2019; Wickham 2019). To compare goodness of model fits with Miller & Thode (2007), Miller *et al.* (2009), and Parks *et al.* (2014), we report the average R^2 value from the cross validation for each of the models. We used the severity calculation derived from the best fitting model from this comparison for all further analyses, which used a 48-day time window and the Relative Burn Ratio (RBR; (Parks *et al.* 2014)) spectral index (ten-fold cross validation $R^2 = 0.806$; first panel of Fig. 2; Supp. Table 1). Example algorithm outputs are shown in Fig. 3.

Using the non-linear relationship between RBR and CBI from the best performing calibration model, we calculated the threshold RBR corresponding to "high-severity" signifying complete or near-complete overstory mortality using the common CBI high-severity lower threshold of 2.25 (i.e., an RBR value of 282.335) (Miller & Thode 2007).

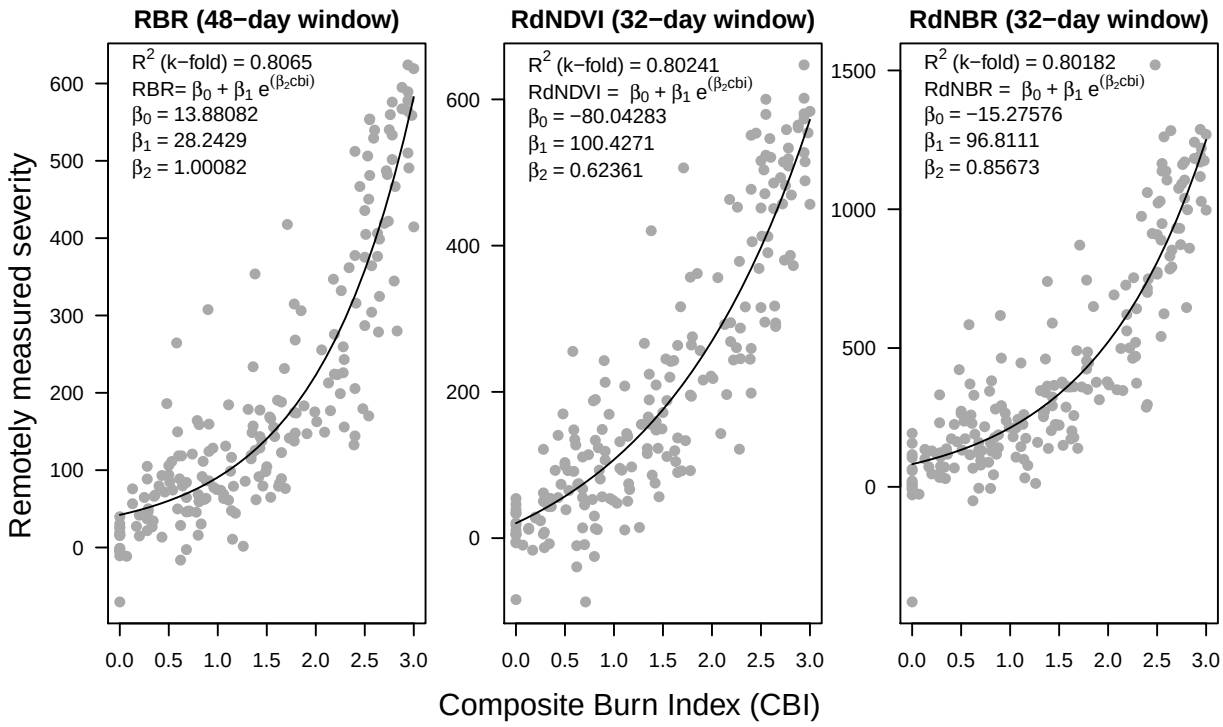

Fig. 2. Three top performing remotely-sensed severity metrics based on ten-fold cross validation (relative burn ratio, 48-day window, bicubic interpolation; relative delta normalized burn ratio, 32-day window, bilinear interpolation; and relative delta normalized difference vegetation index, 48-day window, bilinear interpolation) calculated using new automated image collation algorithms, calibrated to 208 field measures of fire severity (composite burn index). See Supplemental Table 1 for performance of all tested models.

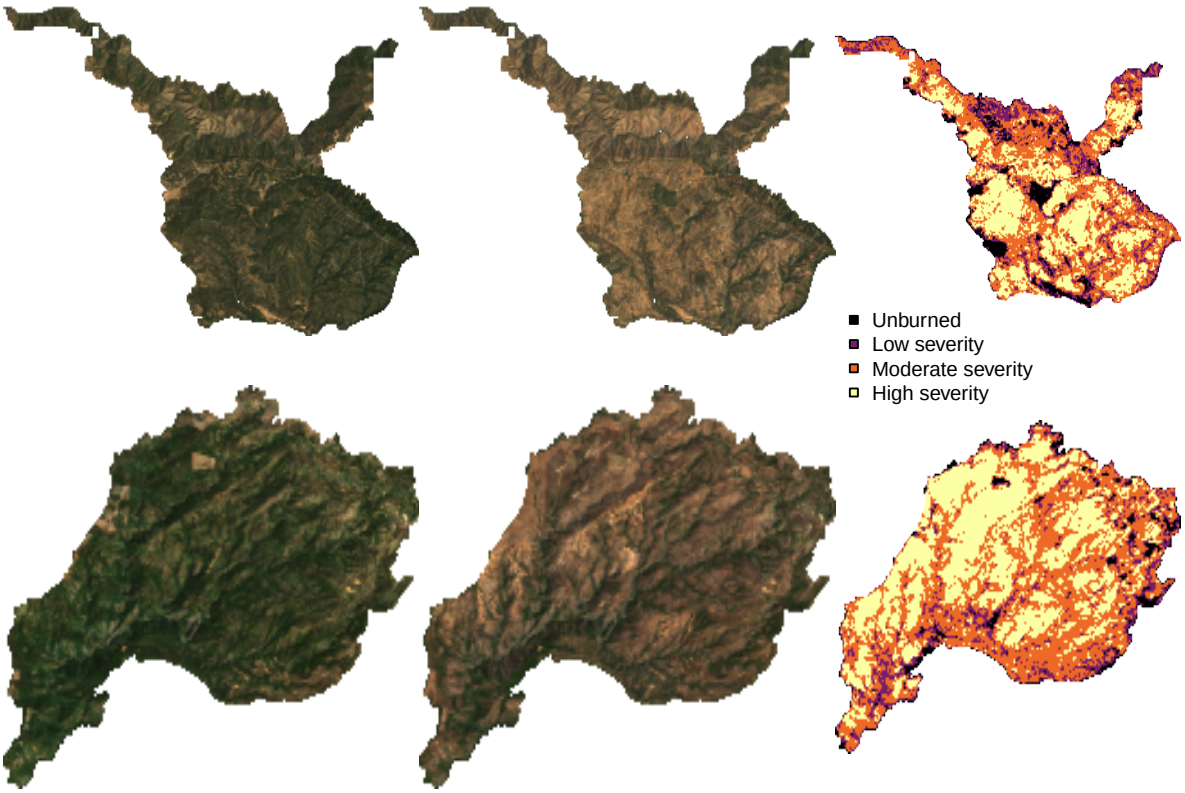

Fig. 3. Example algorithm outputs for the Hamm Fire of 1987 (top half) and the American Fire of 2013 (bottom half) showing: prefire true color composite image (left third), postfire true color composite image (center third), relative burn ratio (RBR) calculation using a 48-day image collation window before the fire and one year later (right third). For visualization purposes, these algorithm outputs have been resampled to a resolution of 100m x 100m from their original resolution of 30 x 30m, and the continous severity index has been binned into severity categories. Data used for analyses were sampled from the outputs at the original resolution.

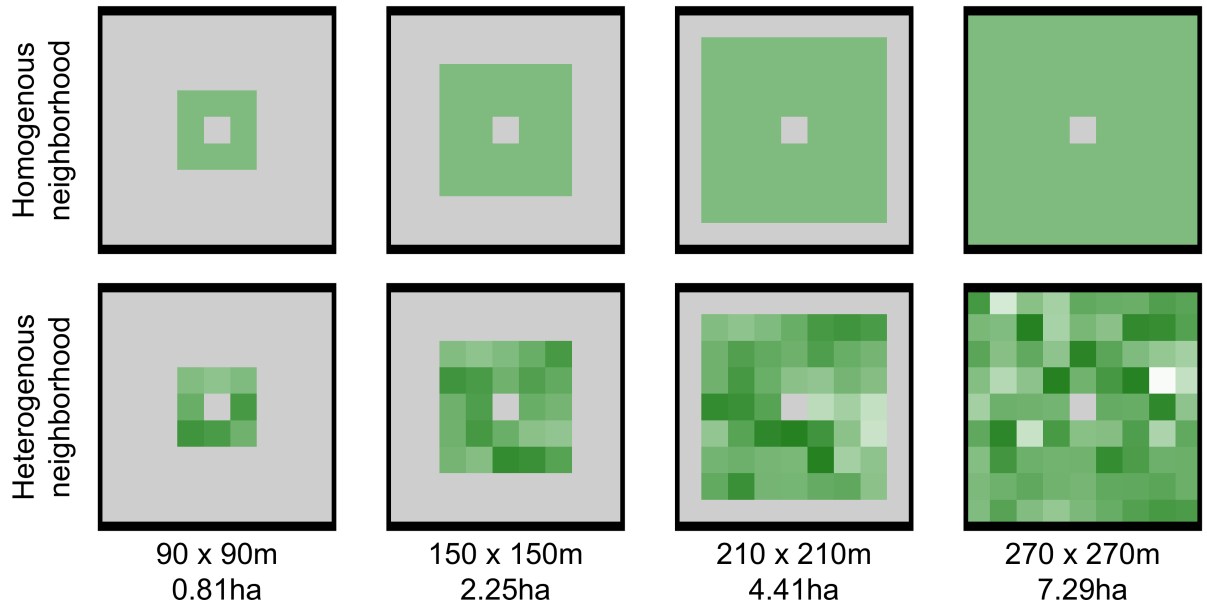

Fig. 4. Example of homogenous forest (top row) and heterogenous forest (bottom row) with the same mean NDVI values (~0.6). Each column represents forest structural variability measured using a different neighborhood size. NDVI is represented by a white to green color gradient, and pixels that are not included in the forest structural variability metric are colored gray.

Remotely sensing local variability in forest structure at broad extents

We used texture analysis to calculate a remotely-sensed measure of local forest variability (Haralick *et al.* 1973; Tuanmu & Jetz 2015). Within a moving square neighborhood window with sides of 90m (3x3 pixels), 150m (5x5 pixels), 210m (7x7 pixels), and 270m (9x9 pixels), we calculated forest variability for each pixel as the standard deviation of the NDVI values of its neighbors (not including itself). NDVI correlates well with foliar biomass, leaf area index, and vegetation cover (Rouse *et al.* 1973), so a higher standard deviation of NDVI within a given local neighborhood corresponds to discontinuous canopy cover and abrupt vegetation edges (see Fig. 4) (Franklin *et al.* 1986). Canopy cover is positively correlated with surface fuel loads including dead and down wood, grasses, and short shrubs (Lydersen *et al.* 2015; Collins *et al.* 2016), which are primarily responsible for initiation and spread of "crowning" fire behavior which kills overstory trees (Stephens *et al.* 2012).

Remote sensing other conditions

Topographic conditions

Elevation data were sourced from the Shuttle Radar Topography Mission (Farr *et al.* 2007), a 1-arc second digital elevation model. Slope and aspect were extracted from the digital elevation model. Per-pixel

topographic roughness was calculated as the standard deviation of elevation values within the same-sized kernels as those used for variability in forest structure (90m, 150m, 210m, and 270m on a side and not including the central pixel). We chose this specific measure of topographic roughness because it directly parallels and accounts for our metric of forest structure variability and because of its use in other studies (Holden *et al.* 2009), though other measures of topographic heterogeneity have been used for fire modeling (Haire & McGarigal 2009; Holden *et al.* 2009; Cansler & McKenzie 2014).

We used the digital elevation model to calculate the potential annual heat load at each pixel, which is an integrated measure of latitude, slope, and a folding transformation of aspect about the northeast-southwest line (McCune & Keon (2002) with correction in McCune (2007); See Supplemental Methods for equations)

Moisture conditions

The modeled 100-hour fuel moisture data were sourced from the gridMET product, a gridded meteorological product with a daily temporal resolution and a 4km x 4km spatial resolution (Abatzoglou 2013). We calculated 100-hour fuel moisture as the median 100-hour fuel moisture for the 3 days prior to the fire. The 100-hour fuel moisture is a correlate of the regional temperature and moisture which integrates the relative humidity, the length of day, and the amount of precipitation in the previous 24 hours. Thus, this measure is sensitive to multiple hot dry days across the 4km x 4km spatial extent of each grid cell, but not to diurnal variation in relative humidity nor to extreme weather events during a fire.

Remote samples

Approximately 100 random points were selected within each FRAP fire perimeter in areas designated as yellow pine/mixed-conifer forest and the values of wildfire severity as well as the values of each covariate were extracted at those points using nearest neighbor interpolation. Using the calibration equation described in Eq. 1 for the best configuration of the remote severity metric, we removed sampled points corresponding to "unburned" area prior to analysis (i.e., below an RBR threshold of 45.097). The random sampling amounted to 56088 total samples across 1008 fires.

Modeling the effect of forest variability on severity

We used a hierarchical logistic regression model (Eq. 2) to assess the probability of high-severity wildfire as a linear combination of the remote metrics described above: prefire NDVI of each pixel, standard deviation of NDVI within a neighborhood (i.e., forest structural variability), the mean NDVI within a neighborhood, 100-hour fuel moisture, potential annual heat load, and topographic roughness. We included two-way interactions

between the structural variability measure and prefire NDVI, neighborhood mean NDVI, and 100-hour fuel moisture. We include the two-way interaction between a pixel's prefire NDVI and its neighborhood mean NDVI to account for structural variability that may arise from contrasts between these variables (e.g., "holes in the forest" vs. "isolated patches"; see Supplemental Fig. 2). We scaled all predictor variables, used weakly-regularizing priors, and estimated an intercept for each individual fire with pooled variance (i.e., a group-level effect of fire).

$$
\begin{aligned}
severity_{i,j} &\sim Bern(\phi_{i,j}) \\
(2)\quad logit(\phi_{i,j}) = &\ \beta_0 + \\
&\ \beta_{\text{nbhd\_stdev\_NDVI}} * \text{nbhd\_stdev\_NDVI}_i + \\
&\ \beta_{\text{prefire\_NDVI}} * \text{prefire\_NDVI}_i + \\
&\ \beta_{\text{nbhd\_mean\_NDVI}} * \text{nbhd\_mean\_NDVI}_i + \\
&\ \beta_{\text{fm100}} * \text{fm100}_i + \\
&\ \beta_{\text{pahl}} * \text{pahl}_i + \\
&\ \beta_{\text{topographic\_roughness}} * \text{topographic\_roughness}_i + \\
&\ \beta_{\text{nbhd\_stdev\_NDVI*fm100}} * \text{nbhd\_stdev\_NDVI}_i * \text{fm100}_i + \\
&\ \beta_{\text{nbhd\_stdev\_NDVI*prefire\_NDVI}} * \text{nbhd\_stdev\_NDVI}_i * \text{prefire\_NDVI}_i + \\
&\ \beta_{\text{nbhd\_stdev\_NDVI*nbhd\_mean\_NDVI}} * \text{nbhd\_stdev\_NDVI}_i * \text{nbhd\_mean\_NDVI}_i + \\
&\ \beta_{\text{nbhd\_mean\_NDVI*prefire\_NDVI}} * \text{nbhd\_mean\_NDVI}_i * \text{prefire\_NDVI}_i + \\
&\ \gamma_j \\
\gamma_j &\sim \mathcal{N}(0, \sigma_{\text{fire}})
\end{aligned}
$$

Assessing the "scale of effect" of forest structure variability

Each neighborhood size (90m, 150m, 210m, 270m on a side) was substituted in turn for the neighborhood standard deviation of NDVI, neighborhood mean NDVI, and terrain ruggedness covariates to generate a candidate set of 4 models. To assess the scale at which these neighborhood-size-dependent effects manifested, we compared the 4 candidate models based on different neighborhood sizes using leave-one-out cross validation (LOO cross validation) (Vehtari *et al.* 2017). We inferred that the neighborhood size window used in the best-performing model reflected the scale at which the forest structure variability effect had the most support (Graham *et al.* 2019).

Statistical software

We used `R` for all statistical analyses (R Core Team 2018). We used the `brms` package to fit mixed effects models in a Bayesian framework which implements the No U-Turn Sampler (NUTS) extension to the Hamiltonian Monte Carlo algorithm (Hoffman & Gelman 2014; Bürkner 2017). We used 4 chains with 3000 samples per chain (1500 warmup samples and 1500 posterior samples) and chain convergence was assessed for each estimated parameter by ensuring Rhat values were less than or equal to 1.01 (Bürkner 2017).

Data availability

All data and analysis code are available via the Open Science Framework (DOI: 10.17605/OSF.IO/27NSR) including a new dataset representing wildfire severity, vegetation characteristics, and regional climate conditions within the perimeters of 1,090 fires from the FRAP database that burned in yellow pine/mixed-conifer forest in the Sierra Nevada, California between 1984 and 2018.

Results

Programmatic assessment of severity

Our programmatic assessment of wildfire severity calibrates as well or better than most other reported methods that often require substantial manual intervention (see review in Edwards *et al.* (2018)). Further, several combinations of remotely sensed severity metrics, time windows, and interpolation methods validate well with the ground-based severity metrics, including those based on NDVI which is calculated using reflectance in shorter wavelengths than those typically used for measuring severity (Fig. 2). The top three configurations of our remotely sensed severity metric are depicted in Fig. 2.

Scale of effect of forest structure variability, topographic roughness, and neighborhood mean NDVI

Tab. 1: Comparison of four models described in Eq. 2 using different neighborhood sizes for calculating forest structural variability (standard deviation of NDVI within the neighborhood), neighborhood mean NDVI, and topographic roughness (standard deviation of elevation within the neighborhood). LOO is a measure of a model's predictive accuracy (with lower values corresponding to more accurate prediction) and is calculated as -2 times the expected log pointwise predictive density (elpd) for a new dataset (Vehtari *et al.* 2017). ΔLOO is the difference between a model's LOO and the lowest LOO in a set of models (i.e., the model with the best predictive accuracy). The Bayesian R^2 is a 'data-based estimate of the proportion of variance explained for new data' (Gelman *et al.* 2018). Note that Bayesian R^2 values are conditional on the model so shouldn't be compared across models, though they can be informative about a single model at a time.

Model	Neighborhood size for variability measure	LOO (-2*elpd)	Δ LOO to best model	SE of Δ LOO	LOO model weight (%)	Bayesian R^2
1	90 x 90m	42364	0	NA	100	0.300
2	150 x 150m	42417	53.17	14.99	0	0.299
3	210 x 210m	42459	94.44	21.35	0	0.299
4	270 x 270m	42491	126.5	25.15	0	0.298

The model with the best out-of-sample prediction accuracy assessed by leave-one-out cross validation was the model fit using the smallest neighborhood size for the variability of forest structure (standard deviation of neighborhood NDVI), the mean of neighborhood NDVI, and the terrain roughness (standard deviation of elevation) (Tab. 1). Model weighting based on the LOO score suggests 100% of the model weight belongs to the model using the smallest neighborhood size window.

Effects of prefire vegetation density, 100-hour fuel moisture, potential annual heat load, and topographic roughness on wildfire severity

We report the results from fitting the model described in Eq. 2 using the smallest neighborhood size (90m x 90m) because this was the best performing model (see above) and because the size and magnitude of estimated coefficients were similar across neighborhood sizes (See Supp. Table 2 for a summary of all parameter estimates for all models).

The strongest influence on the probability of a forested area burning at high-severity was the density of the vegetation, as measured by the prefire NDVI at that central pixel. A greater prefire NDVI led to a greater probability of high-severity fire ($\beta_{\text{prefire\_ndvi}}$ = 1.06; 95% CI: [0.931, 1.192]); Fig. 5). There was a strong negative relationship between 100-hour fuel moisture and wildfire severity such that increasing 100-hour fuel moisture was associated with a reduction in the probability of a high-severity wildfire (β_{fm100} = -0.576; 95%

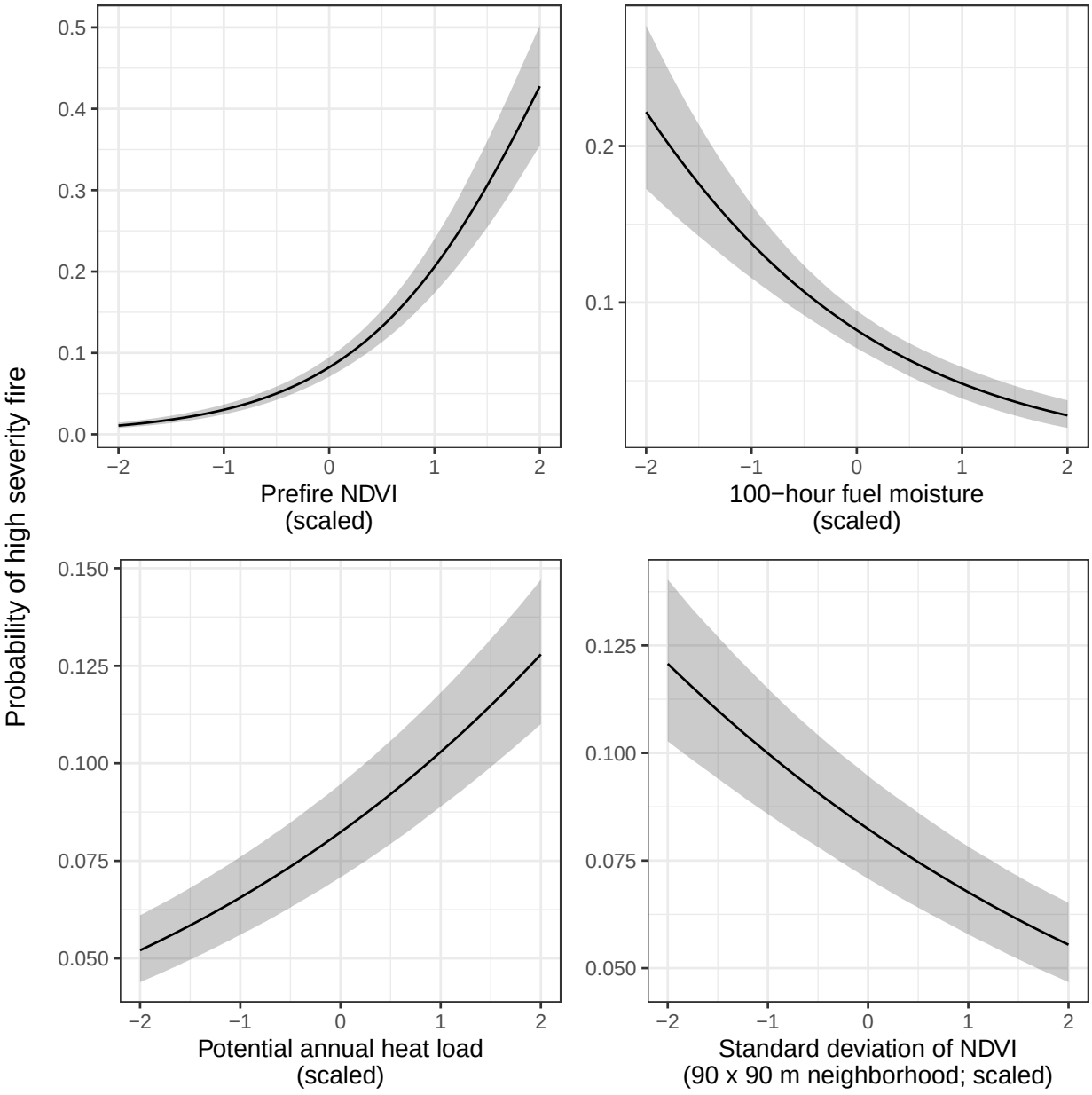

Fig. 5. The main effects and 95% credible intervals of the covariates having the strongest relationships with the probability of high-severity fire. All depicted relationships derive from the model using the 90m x 90m neighborhood size window for neighborhood standard deviation of NDVI, neighborhood mean of NDVI, and topographic roughness, as this was the best performing model of the four neighborhood sizes tested. The effect sizes of these covariates were similar for each neighborhood size tested.

CI: [-0.709, -0.442]) (Fig. 5). Potential annual heat load, which integrates aspect, slope, and latitude, also had a strong positive relationship with the probability of a high-severity fire. Areas that were located on southwest facing sloped terrain at lower latitudes had the highest potential annual heat load, and they were more likely to burn at high-severity (β_{pahl} = 0.246; 95% CI: [0.215, 0.277]) Fig. 5). We found a negative effect of the prefire neighborhood mean NDVI on the probability of a pixel burning at high-severity ($\beta_{\text{nbhd\_mean\_NDVI}}$ = -0.168; 95% CI: [-0.311, -0.028]). This is in contrast to the positive effect of the prefire NDVI of the pixel itself. We found no effect of local topographic roughness on wildfire severity ($\beta_{\text{topographic\_roughness}}$ = 0.002; 95% CI: [-0.029, 0.034]).

There was also a strong negative interaction between the neighborhood mean NDVI and the prefire NDVI of the central pixel ($\beta_{\text{nbhd\_mean\_NDVI*prefire\_NDVI}}$ -0.54; 95% CI: [-0.587, -0.494]).

Effect of variability of vegetation structure on wildfire severity

From the same model, we found strong evidence for a negative effect of variability of vegetation structure on the probability of a high-severity wildfire ($\beta_{\text{nbhd\_stdev\_NDVI}}$ = -0.213; 95% CI: [-0.251, -0.174]); Fig. 5). We also found significant interactions between variability of vegetation structure and prefire NDVI of the central pixel $\beta_{\text{nbhd\_stdev\_NDVI*prefire\_NDVI}}$ = 0.128; 95% CI: [0.031, 0.221]) as well as between variability of vegetation structure and neighborhood mean NDVI ($\beta_{\text{nbhd\_stdev\_NDVI*nbhd\_mean\_NDVI}}$ = -0.115; 95% CI: [-0.206, -0.022]).

Discussion

Broad-extent, fine-grain, spatially-explicit analyses of whole ecosystems are key to illuminating macroecological phenomena such as forest resilience to disturbance (Heffernan *et al.* 2014). We used a powerful, cloud-based geographic information system and data repository, Google Earth Engine, as a 'macroscope' (Beck *et al.* 2012) to study feedbacks between vegetation structure and wildfire disturbance in yellow pine/mixed-conifer forests of California's Sierra Nevada mountain range. With this approach, we reveal and quantify general features of this forest system, and gain deeper insights into the mechanisms underlying its function.

High-severity wildfire in the context of ecological resilience

Wildfire severity can be considered a direct correlate of a forest's resistance– the ease or difficulty with which a disturbance changes the system state (Folke *et al.* 2004; Walker *et al.* 2004). One relevant state change for assessing ecosystem resistance is the loss of its characteristic native biota (Keith *et al.* 2013), which could be

represented as overstory tree mortality (e.g., severity) in a forested system. The same fire behavior in two different forest systems (e.g., old-growth conifer versus young conifer plantation) may have very different abilities to cause overstory mortality (Keeley 2009), which reflects differences in each forest's resistance. Resistance is a key component of resilience (Folke *et al.* 2004; Walker *et al.* 2004) and, in this framework, one manifestation of forest resilience is high resistance to wildfire, whereby some mechanism leads to lower severity when a fire occurs. Here, we show clear evidence that structural heterogeneity fulfills this mechanistic resistance role in dry coniferous systems (Fig. 5). This study thus provides a particularly extensive, large-scale example of an association between local structural heterogeneity and ecosystem resilience, a phenomenon that has been demonstrated in other systems at smaller scales.

These findings do not imply that resistance to fire is the only (or a necessary) path to resilience. For instance, high-severity fire is characteristic of other forest systems such as serotinous lodgepole pine forests in Yellowstone National Park, and is not ordinarily expected to hamper forest regeneration (Turner *et al.* 1997). Our inference that structural variability is a fundamental resilience mechanism in dry coniferous forests is strengthened by its large effect size and our ability to measure the negative feedback phenomenon at relevant spatiotemporal scales: we captured local-scale variability in structure and wildfire severity at broad spatial extents for an extensive set of over 1,000 fires across a 34-year time span.

Factors influencing the probability of high-severity wildfire

We found that the strongest influence on the probability of high-severity wildfire was prefire NDVI. Greater NDVI corresponds to high canopy cover and vegetation density (Rouse *et al.* 1973) which translates directly to live fuel loads in the forest canopy and can increase high-severity fire (Parks *et al.* 2018a). Overstory canopy cover and density also correlate (though weakly) with surface fuel loads (Lydersen *et al.* 2015; Collins *et al.* 2016; Cansler *et al.* 2019), which can play a large role in driving high-severity fire in these forests (Agee 1996). Thus NDVI is likely a strong predictor of fire severity because it is correlated with both surface fuel loads and canopy live fuel density.

We found a strong positive effect of potential annual heat load as well as a strong negative effect of 100-hour fuel moisture, results which corroborates similar studies (Parks *et al.* 2018a). Some work has shown that terrain ruggedness (Haire & McGarigal 2009, @dillon2011; Holden *et al.* 2009; Krawchuk *et al.* 2016) can be an important predictor of wildfire severity, but we found no effect using our measure of local terrain variability. This may be a function of scale– our measures of topographic roughness were more localized than those of studies that found similarly-calculated measures to be an important predictor of severity (Holden *et al.* 2009; Dillon *et al.* 2011). Haire & McGarigal (2009) also found occassional instances where small differences in

topographic roughness had dramatic differences in severity. These sorts of influences on severity would be challenging to detect given that our modeling framework was designed to estimate an overall influence of topographic roughness on fire severity. Also, many different measures of topographic roughness exist (Holden *et al.* 2009), and more could be imagined based on first- and second-order texture of an elevation model that highlight different types of heterogeneity (Haralick *et al.* 1973). An effect of topographic roughness on mean wildfire severity may be better captured by a roughness measure that aligns with the dominant phenomenon driving that effect. Finally, the observed influence of topographic roughness in other studies may have been partitioned in our study as an effect of heterogeneity in local NDVI.

Critically, we found a strong negative effect of forest structural variability on wildfire severity that was opposite in direction but similar in magnitude to the effect of potential annual heat load. Just as the positive effect of NDVI is likely driven by increased fuel loads, the negative effect of variability in NDVI (our measure of structural variability), is likely driven by discontinuity in surface, ladder, and canopy fuels, which can reduce the probability of initiation and spread of tree-killing crown fires (Wagner 1977; Agee 1996; Graham *et al.* 2004; Agee & Skinner 2005). This discontinuity can manifest in a number of ways. For instance, forest patches with similar species compositions but different tree size distributions may disrupt a crown fire's spread from a low to a high crown or vice versa. Our measure of forest structural variability may also reflect intermixed species compositions such as a forested pixel adjacent to a pixel mostly covered by grass, with a grass fire failing to initiate or sustain active crowning behavior that would kill overstory trees. Finally, forest structural variability may also arise with different land cover types in the local neighborhood that influence severity. For instance, exposed bedrock can be a fire refugia and act as a buffer to fire effects for any vegetation rooted within it (Hylander & Johnson 2010). The strong influence of a decreased connectivity of fuels at a local scale suggests that heterogeneity in forest structure may also influence broader-scale wildfire behavior and effects via cross-scale interactions (Peters *et al.* 2004; Rose *et al.* 2017).

Feedback between forest structural variability and wildfire severity

This system-wide inverse relationship between structural variability and wildfire severity closes a feedback that links past and future fire behavior via forest structure. Frequent wildfire in dry coniferous forests generates variable forest structure (North *et al.* 2009; Larson & Churchill 2012; Malone *et al.* 2018), which in turn, as we demonstrate, dampens the severity of future fire. In contrast, exclusion of wildfire homogenizes forest structure and increases the probability that a fire, when it occurs, will produce large, contiguous patches of overstory mortality (Stevens *et al.* 2017; Steel *et al.* 2018). The proportion and spatial configuration of fire severity in fire-prone forests are key determinants of their long-term persistence (Stevens *et al.* 2017;

Steel *et al.* 2018). Lower-severity fire or scattered patches of higher-severity fire reduce the risk of conversion to a non-forest vegetation type (Kemp *et al.* 2016; Stevens-Rumann *et al.* 2018; Walker *et al.* 2018), while prospects for forest regeneration are bleak when high-severity patch sizes are much larger than the natural range of variation for the system (Wagtendonk 2006; Stephens *et al.* 2009; Millar & Stephenson 2015; Coppoletta *et al.* 2016; Miller & Safford 2017; Safford & Stevens 2017; Stevens *et al.* 2017). Thus, the forest-structure-mediated feedback between past and future fire severity underlies the resilience of the Sierra Nevada yellow pine/mixed-conifer system.

Scale of effect of variability in forest structure

We found that the effect of a forest patch's neighborhood characteristics on the probability of high-severity fire was strongest at the smallest neighborhood size that we tested, 90m x 90m. This suggests that the moderating effect of variability in vegetation structure on fire severity is a very local phenomenon. This corroborates work by Safford *et al.* (2012), who found that crown fires (with high tree killing potential) were almost always reduced to surface fires (with low tree killing potential) within 70m of entering an fuel reduction treatment area.

Severity patterns at a landscape scale (e.g., for a whole fire) may represent cross-scale emergences (Heffernan *et al.* 2014) of very local interactions between forest structure and fire behavior. For instance, forest management actions (e.g., prescribed fire, use of wildfire under mild conditions) that reduce fuel loads and increase structural variability can be effective at reducing fire severity across broader spatial extents than the direct footprints of those actions (Graham *et al.* 2004; Stephens *et al.* 2009; Tubbesing *et al.* 2019). Some work suggests that this sort of cross-scale emergence may depend on even broader-scale effects of fire weather, with small-scale variability failing to influence fire behavior under extreme conditions (Peters *et al.* 2004; Lydersen *et al.* 2014), though we did not detect such an interaction between our metric of burning conditions (100-hour fuel moisture) and variability in forest structure.

Correlation between covariates and interactions

Unexpectedly, we found a strong interaction between the prefire NDVI at a pixel and its neighborhood mean NDVI on the probability of high-severity fire. These two variables are strongly correlated (Spearman's $\rho = 0.97$), so the general effect of this interaction is to dampen the dominating effect of prefire NDVI. Thus, though the marginal effect of prefire NDVI on the probability of high-severity fire is still positive and large, its real-world effect might be more comparable to other modeled covariates when including the negative main effect of neighborhood mean NDVI, the negative interaction effect of prefire NDVI and

neighborhood mean NDVI, and their tendency to covary (compare the effect of vegetation density under the common scenario of prefire NDVI and neighborhood mean NDVI increasing or decreasing together: $\beta_{\text{prefire\_ndvi}} + \beta_{\text{nbhd\_mean\_NDVI}} + \beta_{\text{nbhd\_mean\_NDVI*prefire\_NDVI}} = 0.352$, to the effect of 100-hour fuel moisture, which becomes the effect with the greatest magnitude: $\beta_{\text{fm100}} = -0.576$).

In the few cases when prefire NDVI and the neighborhood mean NDVI contrast, there is an overall effect of increasing the probability of high-severity fire. When prefire NDVI at the central pixel is high and the neighborhood NDVI is low (e.g., an isolated vegetation patch; Supplemental Fig. 2), the probability of high-severity fire is expected to dramatically increase. When prefire NDVI at the central pixel is low and the neighborhood NDVI is high (e.g., a hole in the center of an otherwise dense forest; Supplemental Fig. 2), the probability of high-severity fire at that central pixel is still expected to be fairly high even though there is limited vegetation density (see Supplemental Fig. 2). In these forest NDVI datasets, when these variables do decouple, they tend to do so in the "hole in the forest" case and lead to a greater probability of high-severity fire at the central pixel despite the lower vegetation density there. This can perhaps be explained if the consistently high vegetation density in a local neighborhood– itself more likely to burn at high-severity– exerts a contagious effect on the central pixel, raising its probability of burning at high-severity regardless of how much fuel might be there to burn.

A programmatic approach to remotely sensing wildfire severity

We developed an approach to calculating wildfire severity leveraging the cloud-based data catalog, the large parallel processing system, and the distribution of computation tasks in Google Earth Engine to enable rapid high-throughput analyses of earth observation data (Gorelick *et al.* 2017; Parks *et al.* 2018b, 2019). Our programmatic assessment of wildfire severity across the 1008 Sierra Nevada yellow pine/mixed-conifer fires in the FRAP perimeter database, which enabled consistent assessment of severity for a broad representation of fires including smaller events (Randerson *et al.* 2012). We found that the relative burn ratio (RBR) calculated using prefire Landsat images collected over a 48-day period prior to the fire and postfire Landsat images collected over a 48-day period one year after the prefire images validated the best with ground-based severity measurements (composite burn index; CBI). Further, we found that this programmatic approach was robust to a wide range of severity metrics, time windows, and interpolation techniques.

We echo the conclusion of Zhu *et al.* (2006) that the validation of differences between pre- and postfire NDVI to field-measured severity data, which uses near infrared reflectance, is comparable to validation using more commonly used severity metrics (e.g., RdNBR and RBR) that rely on short wave infrared reflectance. One immediately operational implication of this is that the increasing availability of low-cost small unhumanned

aerial systems (sUAS a.k.a. drones) and near-infrared-detecting imagers (e.g., those used for agriculture monitoring) may be used to reliably assess wildfire severity at very high spatial resolutions.

Conclusions

Theory and empirical work suggest a general link between forest structural heterogeneity and resilience. Here we find strong evidence with a large-scale study that, across large areas of forest, variable forest structure generally makes yellow pine/mixed-conifer forest in the Sierra Nevada more resistant to inevitable wildfire disturbance. It has been well-documented that frequent, low-severity wildfire maintains forest structural variability. Here, we demonstrate a system-wide reciprocal effect suggesting that greater local-scale variability of vegetation structure makes fire-prone, dry forests more resilient to wildfire and may increase the probability of their long-term persistence.

Acknowledgements

We thank Connie Millar, Derek Young, and Meagan Oldfather for valuable comments about this work and we also thank the community of Google Earth Engine developers for prompt and helpful insights about the platform. We thank four anonymous reviewers for their helpful comments on the manuscript. Funding was provided by NSF Graduate Research Fellowship Grant #DGE- 1321845 Amend. 3 (to MJK).

References

1.

Abatzoglou, J.T. (2013). Development of gridded surface meteorological data for ecological applications and modelling. *International Journal of Climatology*, 33, 121–131.

2.

Abatzoglou, J.T. & Williams, A.P. (2016). Impact of anthropogenic climate change on wildfire across western U.S. Forests. *Proceedings of the National Academy of Sciences*, 113, 11770–11775.

3.

Ackerly, D.D., Loarie, S.R., Cornwell, W.K., Weiss, S.B., Hamilton, H. & Branciforte, R. *et al.* (2010). The geography of climate change: Implications for conservation biogeography. *Diversity and Distributions*, 16, 476–487.

4.

Agashe, D. (2009). The stabilizing effect of intraspecific genetic variation on population dynamics in novel and ancestral habitats. *The American Naturalist*, 174, 255–267.

5.

Agee, J.K. (1996). The influence of forest structure on fire behavior. *17th Forest Vegetation Management Conference*, 17.

6.

Agee, J.K. & Skinner, C.N. (2005). Basic principles of forest fuel reduction treatments. *Forest Ecology and Management*, 211, 83–96.

7.

Baskett, M.L., Gaines, S.D. & Nisbet, R.M. (2009). Symbiont diversity may help coral reefs survive moderate climate change. *Ecological Applications*, 19, 3–17.

8.

Beck, J., Ballesteros-Mejia, L., Buchmann, C.M., Dengler, J., Fritz, S.A. & Gruber, B. *et al.* (2012). What's on the horizon for macroecology? *Ecography*, 35, 673–683.

9.

Bessie, W.C. & Johnson, E.A. (1995). The relative importance of fuels and weather on fire behavior in subalpine forests. *Ecology*, 76, 747–762.

10.

Bürkner, P.-C. (2017). **brms**: An *R* package for bayesian multilevel models using *Stan*. *Journal of Statistical Software*, 80.

11.

Cadotte, M., Albert, C.H. & Walker, S.C. (2013). The ecology of differences: Assessing community assembly with trait and evolutionary distances. *Ecology Letters*, 16, 1234–1244.

12.

Cansler, C.A. & McKenzie, D. (2012). How robust are burn severity indices when applied in a new region? Evaluation of alternate field-based and remote-sensing methods. *Remote Sensing*, 4, 456–483.

13.

Cansler, C.A. & McKenzie, D. (2014). Climate, fire size, and biophysical setting control fire severity and spatial pattern in the northern Cascade Range, USA. *Ecological Applications*, 24, 1037–1056.

14.

Cansler, C.A., Swanson, M.E., Furniss, T.J., Larson, A.J. & Lutz, J.A. (2019). Fuel dynamics after reintroduced fire in an old-growth Sierra Nevada mixed-conifer forest. *Fire Ecology*, 15, 16.

15.

Chesson, P. (2000). Mechanisms of maintenance of species diversity. *Annual Review of Ecology and Systematics*, 31, 343–366.

16.

Clark, J.S., Iverson, L., Woodall, C.W., Allen, C.D., Bell, D.M. & Bragg, D.C. *et al.* (2016). The impacts of increasing drought on forest dynamics, structure, and biodiversity in the United States. *Global Change Biology*, 22, 2329–2352.

17.

Collins, B.M., Lydersen, J.M., Fry, D.L., Wilkin, K., Moody, T. & Stephens, S.L. (2016). Variability in vegetation and surface fuels across mixed-conifer-dominated landscapes with over 40 years of natural fire. *Forest Ecology and Management*, 381, 74–83.

18.

Collins, B.M. & Roller, G.B. (2013). Early forest dynamics in stand-replacing fire patches in the northern Sierra Nevada, California, USA. *Landscape Ecology*, 28, 1801–1813.

19.

Coppoletta, M., Merriam, K.E. & Collins, B.M. (2016). Post-fire vegetation and fuel development influences fire severity patterns in reburns. *Ecological Applications*, 26, 686–699.

20.

Crowther, T.W., Glick, H.B., Covey, K.R., Bettigole, C., Maynard, D.S. & Thomas, S.M. *et al.* (2015). Mapping tree density at a global scale. *Nature*, 525, 201–205.

21.

D'Amato, A.W., Bradford, J.B., Fraver, S. & Palik, B.J. (2013). Effects of thinning on drought vulnerability and climate response in north temperate forest ecosystems. *Ecological Applications*, 23, 1735–1742.

22.

Davis, K.T., Dobrowski, S.Z., Higuera, P.E., Holden, Z.A., Veblen, T.T. & Rother, M.T. *et al.* (2019). Wildfires and climate change push low-elevation forests across a critical climate threshold for tree regeneration. *PNAS*, 201815107.

23.

525 Dillon, G.K., Holden, Z.A., Morgan, P., Crimmins, M.A., Heyerdahl, E.K. & Luce, C.H. (2011). Both
526 topography and climate affected forest and woodland burn severity in two regions of the western U.S., 1984
527 to 2006. *Ecosphere*, 2, art130.

528 24.

529 Edwards, A.C., Russell-Smith, J. & Maier, S.W. (2018). A comparison and validation of satellite-derived fire
530 severity mapping techniques in fire prone north Australian savannas: Extreme fires and tree stem mortality.
531 *Remote Sensing of Environment*, 206, 287–299.

532 25.

533 Eidenshink, J., Schwind, B., Brewer, K., Zhu, Z.-L., Quayle, B. & Howard, S. (2007). A project for monitoring
534 trends in burn severity. *Fire Ecology*, 3, 3–21.

535 26.

536 Farr, T.G., Rosen, P.A., Caro, E., Crippen, R., Duren, R. & Hensley, S. *et al.* (2007). The shuttle radar
537 topography mission. *Reviews of Geophysics*, 45.

538 27.

539 Folke, C., Carpenter, S., Walker, B., Scheffer, M., Elmqvist, T. & Gunderson, L. *et al.* (2004). Regime shifts,
540 resilience, and biodiversity in ecosystem management. *Annual Review of Ecology, Evolution, and Systematics*,
541 3, 557–581.

542 28.

543 Fox, J.M. & Whitesides, G.M. (2015). Warning signals for eruptive events in spreading fires. *Proceedings of*
544 *the National Academy of Sciences*, 112, 2378–2383.

545 29.

546 Franklin, J., Logan, T., Woodcock, C. & Strahler, A. (1986). Coniferous forest classification and inventory
547 using Landsat and digital terrain data. *IEEE Transactions on Geoscience and Remote Sensing*, GE-24,
548 139–149.

549 30.

550 Fried, J.S., Torn, M.S. & Mills, E. (2004). The impact of climate change on wildfire severity: A regional
551 forecast for Northern California. *Climatic Change*, 64, 169–191.

552 31.

553 Gazol, A. & Camarero, J.J. (2016). Functional diversity enhances silver fir growth resilience to an extreme
554 drought. *Journal of Ecology*, 104, 1063–1075.

32.

Gelman, A., Goodrich, B., Gabry, J. & Vehtari, A. (2018). R-squared for Bayesian regression models. *The American Statistician*, 1–6.

33.

Gorelick, N., Hancher, M., Dixon, M., Ilyushchenko, S., Thau, D. & Moore, R. (2017). Google Earth Engine: Planetary-scale geospatial analysis for everyone. *Remote Sensing of Environment*, 202, 18–27.

34.

Graham, L.J., Spake, R., Gillings, S., Watts, K. & Eigenbrod, F. (2019). Incorporating fine-scale environmental heterogeneity into broad-extent models. *Methods in Ecology and Evolution*, 10, 767–778.

35.

Graham, R.T., McCaffrey, S. & Jain, T.B. (2004). *Science basis for changing forest structure to modify wildfire behavior and severity* (No. RMRS-GTR-120). U.S. Department of Agriculture, Forest Service, Rocky Mountain Research Station, Ft. Collins, CO.

36.

Haire, S.L. & McGarigal, K. (2009). Changes in fire severity across gradients of climate, fire size, and topography: A landscape ecological perspective. *fire ecol*, 5, 86–103.

37.

Hansen, M.C., Potapov, P.V., Moore, R., Hancher, M., Turubanova, S.A. & Tyukavina, A. *et al.* (2013). High-resolution global maps of 21st-century forest cover change. *Science*, 342, 850–853.

38.

Haralick, R.M., Shanmugam, K. & Dinstein, I. (1973). Textural features for image classification. *IEEE Transactions on Systems, Man, and Cybernetics*, SMC-3, 610–621.

39.

Heffernan, J.B., Soranno, P.A., Angilletta, M.J., Buckley, L.B., Gruner, D.S. & Keitt, T.H. *et al.* (2014). Macrosystems ecology: Understanding ecological patterns and processes at continental scales. *Frontiers in Ecology and the Environment*, 12, 5–14.

40.

Henry, L. & Wickham, H. (2019). *Purrr: Functional programming tools.*

41.

Hessburg, P.F., Miller, C.L., Povak, N.A., Taylor, A.H., Higuera, P.E. & Prichard, S.J. *et al.* (2019). Climate,

environment, and disturbance history govern resilience of western North American forests. *Front. Ecol. Evol.*, 7.

42.

Higuera, P.E., Metcalf, A.L., Miller, C., Buma, B., McWethy, D.B. & Metcalf, E.C. *et al.* (2019). Integrating subjective and objective dimensions of resilience in fire-prone landscapes. *BioScience*, 69, 379–388.

43.

Hoffman, M.D. & Gelman, A. (2014). The No-U-Turn Sampler: Adaptively setting path lengths in Hamiltonian Monte Carlo. *Journal of Machine Learning Research*, 15, 31.

44.

Holden, Z.A., Morgan, P. & Evans, J.S. (2009). A predictive model of burn severity based on 20-year satellite-inferred burn severity data in a large southwestern US wilderness area. *Forest Ecology and Management*, 258, 2399–2406.

45.

Holling, C.S. (1973). Resilience and stability of ecological systems. *Annual Review of Ecology and Systematics*, 1–23.

46.

Hylander, K. & Johnson, S. (2010). In situ survival of forest bryophytes in small-scale refugia after an intense forest fire. *Journal of Vegetation Science*, 21, 1099–1109.

47.

JepsonFloraProject (Ed.). (2016). *Jepson eFlora*.

48.

Kane, V.R., Cansler, C.A., Povak, N.A., Kane, J.T., McGaughey, R.J. & Lutz, J.A. *et al.* (2015). Mixed severity fire effects within the Rim fire: Relative importance of local climate, fire weather, topography, and forest structure. *Forest Ecology and Management*, 358, 62–79.

49.

Keeley, J.E. (2009). Fire intensity, fire severity and burn severity: A brief review and suggested usage. *International Journal of Wildland Fire*, 18, 116.

50.

Keith, D.A., Rodríguez, J.P., Rodríguez-Clark, K.M., Nicholson, E., Aapala, K. & Alonso, A. *et al.* (2013). Scientific foundations for an IUCN red list of ecosystems. *PLoS ONE*, 8, e62111.

615 51.

616 Kemp, K.B., Higuera, P.E. & Morgan, P. (2016). Fire legacies impact conifer regeneration across environmental
617 gradients in the U.S. Northern Rockies. *Landscape Ecol*, 31, 619–636.

618 52.

619 Key, C.H. & Benson, N.C. (2006). Landscape assessment (LA): Sampling and analysis methods, 55.

620 53.

621 Kotliar, N.B. & Wiens, J.A. (1990). Multiple scales of patchiness and patch structure: A hierarchical
622 framework for the study of heterogeneity. *Oikos*, 59, 253.

623 54.

624 Krawchuk, M.A., Haire, S.L., Coop, J., Parisien, M.-A., Whitman, E. & Chong, G. *et al.* (2016). Topographic
625 and fire weather controls of fire refugia in forested ecosystems of northwestern North America. *Ecosphere*, 7,
626 e01632.

627 55.

628 Larson, A.J. & Churchill, D. (2012). Tree spatial patterns in fire-frequent forests of western North America,
629 including mechanisms of pattern formation and implications for designing fuel reduction and restoration
630 treatments. *Forest Ecology and Management*, 267, 74–92.

631 56.

632 Lenoir, J., Graae, B.J., Aarrestad, P.A., Alsos, I.G., Armbruster, W.S. & Austrheim, G. *et al.* (2013). Local
633 temperatures inferred from plant communities suggest strong spatial buffering of climate warming across
634 Northern Europe. *Global Change Biology*, 19, 1470–1481.

635 57.

636 Lydersen, J.M., Collins, B.M., Knapp, E.E., Roller, G.B. & Stephens, S. (2015). Relating fuel loads to
637 overstorey structure and composition in a fire-excluded Sierra Nevada mixed conifer forest. *International*
638 *Journal of Wildland Fire*, 24, 484.

639 58.

640 Lydersen, J.M., North, M.P. & Collins, B.M. (2014). Severity of an uncharacteristically large wildfire, the
641 Rim Fire, in forests with relatively restored frequent fire regimes. *Forest Ecology and Management*, 328,
642 326–334.

643 59.

644 Malone, S., Fornwalt, P., Battaglia, M., Chambers, M., Iniguez, J. & Sieg, C. (2018). Mixed-severity fire

fosters heterogeneous spatial patterns of conifer regeneration in a dry conifer forest. *Forests*, 9, 45.

60.

van Mantgem, P.J., Caprio, A.C., Stevenson, N.L. & Das, A.J. (2016). Does prescribed fire promote resistance to drought in low elevation forests of the Sierra Nevada, California, USA? *Fire Ecology*, 12, 13–25.

61.

Masek, J., Vermote, E., Saleous, N., Wolfe, R., Hall, F. & Huemmrich, K. *et al.* (2006). A Landsat surface reflectance dataset for North America, 19902000. *IEEE Geoscience and Remote Sensing Letters*, 3, 68–72.

62.

McCune, B. (2007). Improved estimates of incident radiation and heat load using non- parametric regression against topographic variables. *Journal of Vegetation Science*, 18, 751–754.

63.

McCune, B. & Keon, D. (2002). Equations for potential annual direct incident radiation and heat load. *Journal of Vegetation Science*, 13, 603–606.

64.

McKenzie, D. & Kennedy, M.C. (2011). Scaling laws and complexity in fire regimes. In: *The Landscape Ecology of Fire* (eds. McKenzie, D., Miller, C. & Falk, D.A.). Springer Netherlands, Dordrecht, pp. 27–49.

65.

McKenzie, D. & Kennedy, M.C. (2012). Power laws reveal phase transitions in landscape controls of fire regimes. *Nature Communications*, 3, 726.

66.

McWethy, D.B., Schoennagel, T., Higuera, P.E., Krawchuk, M., Harvey, B.J. & Metcalf, E.C. *et al.* (2019). Rethinking resilience to wildfire. *Nat Sustain*, 1–8.

67.

Millar, C.I. & Stephenson, N.L. (2015). Temperate forest health in an era of emerging megadisturbance. *Science*, 349, 823–826.

68.

Miller, J.D., Knapp, E.E., Key, C.H., Skinner, C.N., Isbell, C.J. & Creasy, R.M. *et al.* (2009). Calibration and validation of the relative differenced Normalized Burn Ratio (RdNBR) to three measures of fire severity in the Sierra Nevada and Klamath Mountains, California, USA. *Remote Sensing of Environment*, 113, 645–656.

69.

675 Miller, J.D. & Safford, H. (2012). Trends in wildfire severity: 1984 to 2010 in the Sierra Nevada, Modoc
676 Plateau, and Southern Cascades, California, U.S.A. *Fire Ecology*, 8, 41–57.

677 70.

678 Miller, J.D. & Safford, H.D. (2017). Corroborating evidence of a pre-Euro-American low- to moderate-severity
679 fire regime in yellow pineMixed conifer forests of the Sierra Nevada, California, USA. *Fire Ecology*, 13, 58–90.

680 71.

681 Miller, J.D., Skinner, C.N., Safford, H.D., Knapp, E.E. & Ramirez, C.M. (2012). Trends and causes of
682 severity, size, and number of fires in northwestern California, USA. *Ecological Applications*, 22, 184–203.

683 72.

684 Miller, J.D. & Thode, A.E. (2007). Quantifying burn severity in a heterogeneous landscape with a relative
685 version of the delta Normalized Burn Ratio (dNBR). *Remote Sensing of Environment*, 109, 66–80.

686 73.

687 Moritz, M.A., Morais, M.E., Summerell, L.A., Carlson, J.M. & Doyle, J. (2005). Wildfires, complexity, and
688 highly optimized tolerance. *Proceedings of the National Academy of Sciences*, 102, 17912–17917.

689 74.

690 North, M., Stine, P., O'Hara, K., Zielinski, W. & Stephens, S. (2009). *An ecosystem management strategy for*
691 *Sierran mixed-conifer forests* (No. PSW-GTR-220). U.S. Department of Agriculture, Forest Service, Pacific
692 Southwest Research Station, Albany, CA.

693 75.

694 Parks, S.A., Holsinger, L.M., Koontz, M.J., Collins, L., Whitman, E. & Parisien, M.-A. *et al.* (2019). Giving
695 ecological meaning to satellite-derived fire severity metrics across North American forests. *Remote Sensing*,
696 11, 1735.

697 76.

698 Parks, S.A., Holsinger, L.M., Panunto, M.H., Jolly, W.M., Dobrowski, S.Z. & Dillon, G.K. (2018a). High-
699 severity fire: Evaluating its key drivers and mapping its probability across western U.S. Forests. *Environmental*
700 *Research Letters*, 13, 044037.

701 77.

702 Parks, S., Dillon, G. & Miller, C. (2014). A new metric for quantifying burn severity: The Relativized Burn
703 Ratio. *Remote Sensing*, 6, 1827–1844.

704 78.

705 Parks, S., Holsinger, L., Voss, M., Loehman, R. & Robinson, N. (2018b). Mean composite fire severity metrics
706 computed with Google Earth Engine offer improved accuracy and expanded mapping potential. *Remote*
707 *Sensing*, 10, 879.

708 79.

709 Parsons, R.A., Linn, R.R., Pimont, F., Hoffman, C., Sauer, J. & Winterkamp, J. *et al.* (2017). Numerical
710 investigation of aggregated fuel spatial pattern impacts on fire behavior. *Land*, 6, 43.

711 80.

712 Peters, D.P.C., Pielke, R.A., Bestelmeyer, B.T., Allen, C.D., Munson-McGee, S. & Havstad, K.M. (2004).
713 Cross-scale interactions, nonlinearities, and forecasting catastrophic events. *Proceedings of the National*
714 *Academy of Sciences*, 101, 15130–15135.

715 81.

716 Prichard, S.J. & Kennedy, M.C. (2014). Fuel treatments and landform modify landscape patterns of burn
717 severity in an extreme fire event. *Ecological Applications*, 24, 571–590.

718 82.

719 Questad, E.J. & Foster, B.L. (2008). Coexistence through spatio-temporal heterogeneity and species sorting
720 in grassland plant communities. *Ecology Letters*, 11, 717–726.

721 83.

722 Randerson, J.T., Chen, Y., Werf, G.R. van der, Rogers, B.M. & Morton, D.C. (2012). Global burned area
723 and biomass burning emissions from small fires. *Journal of Geophysical Research: Biogeosciences*, 117.

724 84.

725 R Core Team. (2018). *R: A language and environment for statistical computing*. R Foundation for Statistical
726 Computing, Vienna, Austria.

727 85.

728 Reusch, T.B.H., Ehlers, A., Hammerli, A. & Worm, B. (2005). Ecosystem recovery after climatic extremes
729 enhanced by genotypic diversity. *Proceedings of the National Academy of Sciences*, 102, 2826–2831.

730 86.

731 Reyer, C.P.O., Brouwers, N., Rammig, A., Brook, B.W., Epila, J. & Grant, R.F. *et al.* (2015a). Forest
732 resilience and tipping points at different spatio-temporal scales: Approaches and challenges. *Journal of*
733 *Ecology*, 103, 5–15.

734 87.

735 Reyer, C.P., Rammig, A., Brouwers, N. & Langerwisch, F. (2015b). Forest resilience, tipping points and
736 global change processes. *Journal of Ecology*, 103, 1–4.

737 88.

738 Rose, K.C., Graves, R.A., Hansen, W.D., Harvey, B.J., Qiu, J. & Wood, S.A. *et al.* (2017). Historical
739 foundations and future directions in macrosystems ecology. *Ecology Letters*, 20, 147–157.

740 89.

741 Rouse, W., Haas, R.H., Deering, W. & Schell, J.A. (1973). *Monitoring the vernal advancement and*
742 *retrogradation (green wave effect) of natural vegetation* (Type II Report No. RSC 1978-2). Goddard Space
743 Flight Center, Greenbelt, MD, USA.

744 90.

745 Safford, H.D. & Stevens, J.T. (2017). *Natural range of variation for yellow pine and mixed-conifer forests*
746 *in the Sierra Nevada, Southern Cascades, and Modoc and Inyo National Forests, California, USA* (No.
747 PSW-GTR-256).

748 91.

749 Safford, H., Stevens, J., Merriam, K., Meyer, M. & Latimer, A. (2012). Fuel treatment effectiveness in
750 California yellow pine and mixed conifer forests. *Forest Ecology and Management*, 274, 17–28.

751 92.

752 Scheffer, M. (2009). *Critical Transitions in Nature and Society*. Princeton University Press.

753 93.

754 Schoennagel, T., Balch, J.K., Brenkert-Smith, H., Dennison, P.E., Harvey, B.J. & Krawchuk, M.A. *et al.*
755 (2017). Adapt to more wildfire in western North American forests as climate changes. *Proceedings of the*
756 *National Academy of Sciences*, 114, 4582–4590.

757 94.

758 Scholl, A.E. & Taylor, A.H. (2010). Fire regimes, forest change, and self-organization in an old-growth
759 mixed-conifer forest, Yosemite National Park, USA. *Ecological Applications*, 20, 362–380.

760 95.

761 Scott, J.H. & Reinhardt, E.D. (2001). *Assessing crown fire potential by linking models of surface and crown*
762 *fire behavior* (No. RMRS-RP-29). U.S. Department of Agriculture, Forest Service, Rocky Mountain Research
763 Station, Ft. Collins, CO.

764 96.

765 Seidl, R., Spies, T.A., Peterson, D.L., Stephens, S.L. & Hicke, J.A. (2016). Searching for resilience: Addressing
766 the impacts of changing disturbance regimes on forest ecosystem services. *J Appl Ecol*, 53, 120–129.

767 97.

768 Sikkink, P.G., Dillon, G.K., Keane, R.E., Morgan, P., Karau, E.C. & Holden, Z.A. *et al.* (2013). Composite
769 Burn Index (CBI) data and field photos collected for the FIRESEV project, western United States.

770 98.

771 Steel, Z.L., Koontz, M.J. & Safford, H.D. (2018). The changing landscape of wildfire: Burn pattern trends
772 and implications for California's yellow pine and mixed conifer forests. *Landscape Ecology*, 33, 1159–1176.

773 99.

774 Stephens, S.L., Fry, D.L. & Franco-Vizcaíno, E. (2008). Wildfire and spatial patterns in forests in Northwestern
775 Mexico: The United States wishes it had similar fire problems. *Ecology and Society*, 13.

776 100.

777 Stephens, S.L., McIver, J.D., Boerner, R.E.J., Fettig, C.J., Fontaine, J.B. & Hartsough, B.R. *et al.* (2012).
778 The effects of forest fuel-reduction treatments in the United States. *BioScience*, 62, 549–560.

779 101.

780 Stephens, S.L., Moghaddas, J.J., Edminster, C., Fiedler, C.E., Haase, S. & Harrington, M. *et al.* (2009). Fire
781 treatment effects on vegetation structure, fuels, and potential fire severity in western U.S. Forests. *Ecological*
782 *Applications*, 19, 305–320.

783 102.

784 Stevens, J.T., Collins, B.M., Miller, J.D., North, M.P. & Stephens, S.L. (2017). Changing spatial patterns of
785 stand-replacing fire in California conifer forests. *Forest Ecology and Management*, 406, 28–36.

786 103.

787 Stevens-Rumann, C.S., Kemp, K.B., Higuera, P.E., Harvey, B.J., Rother, M.T. & Donato, D.C. *et al.* (2018).
788 Evidence for declining forest resilience to wildfires under climate change. *Ecology Letters*, 21, 243–252.

789 104.

790 Stevens-Rumann, C.S., Prichard, S.J., Strand, E.K. & Morgan, P. (2016). Prior wildfires influence burn
791 severity of subsequent large fires. *Canadian Journal of Forest Research*, 46, 1375–1385.

792 105.

793 Sugihara, N.G., Wagtendonk, J.W.V., Fites-Kaufman, J., Shaffer, K.E. & Thode, A.E. (2006). *Fire in*
794 *California's Ecosystems*. University of California Press.

795 106.

796 Tilman, D. (1994). Competition and biodiversity in spatially structured habitats. *Ecology*, 75, 2–16.

797 107.

798 Trumbore, S., Brando, P. & Hartmann, H. (2015). Forest health and global change. *Science*, 349, 814–818.

799 108.

800 Tuanmu, M.-N. & Jetz, W. (2015). A global, remote sensing-based characterization of terrestrial habitat
801 heterogeneity for biodiversity and ecosystem modelling: Global habitat heterogeneity. *Global Ecology and*
802 *Biogeography*, 24, 1329–1339.

803 109.

804 Tubbesing, C.L., Fry, D.L., Roller, G.B., Collins, B.M., Fedorova, V.A. & Stephens, S.L. *et al.* (2019).
805 Strategically placed landscape fuel treatments decrease fire severity and promote recovery in the northern
806 Sierra Nevada. *Forest Ecology and Management*, 436, 45–55.

807 110.

808 Turner, M.G., Donato, D.C. & Romme, W.H. (2013). Consequences of spatial heterogeneity for ecosystem
809 services in changing forest landscapes: Priorities for future research. *Landscape Ecology*, 28, 1081–1097.

810 111.

811 Turner, M.G. & Romme, W.H. (1994). Landscape dynamics in crown fire ecosystems. *Landscape Ecol*, 9,
812 59–77.

813 112.

814 Turner, M.G., Romme, W.H., Gardner, R.H. & Hargrove, W.W. (1997). Effects of fire size and pattern on
815 early succession in Yellowstone National Park. *Ecological Monographs*, 67, 411.

816 113.

817 USGS. (2017a). Landsat 4-7 Surface Reflectance (LEDAPS) Product Guide, 41.

818 114.

819 USGS. (2017b). Landsat 8 Surface Reflectance Code (LASRC) Product Guide, 40.

820 115.

821 Vehtari, A., Gelman, A. & Gabry, J. (2017). Practical Bayesian model evaluation using leave-one-out
822 cross-validation and WAIC. *Statistics and Computing*, 27, 1413–1432.

823 116.

824 Vermote, E., Justice, C., Claverie, M. & Franch, B. (2016). Preliminary analysis of the performance of the

825 Landsat 8/OLI land surface reflectance product. *Remote Sensing of Environment*, 185, 46–56.

826 117.

827 Virah-Sawmy, M., Gillson, L. & Willis, K.J. (2009). How does spatial heterogeneity influence resilience to
828 climatic changes? Ecological dynamics in southeast Madagascar. *Ecological Monographs*, 79, 557–574.

829 118.

830 Wagner, C.E.V. (1977). Conditions for the start and spread of crown fire. *Can. J. For. Res.*, 7, 23–34.

831 119.

832 Wagtendonk, J.W.V. (2006). *Fire as a Physical Process*. University of California Press.

833 120.

834 Walker, B., Holling, C.S., Carpenter, S.R. & Kinzig, A.P. (2004). Resilience, adaptability, and transformability
835 in social-ecological systems. *Ecology and Society*, 9.

836 121.

837 Walker, R.B., Coop, J.D., Parks, S.A. & Trader, L. (2018). Fire regimes approaching historic norms reduce
838 wildfire-facilitated conversion from forest to non-forest. *Ecosphere*, 9, e02182.

839 122.

840 Welch, K.R., Safford, H.D. & Young, T.P. (2016). Predicting conifer establishment post wildfire in mixed
841 conifer forests of the North American Mediterranean-climate zone. *Ecosphere*, 7, e01609.

842 123.

843 Wickham, H. (2019). *Modelr: Modelling functions that work with the pipe*.

844 124.

845 Williams, A.P., Allen, C.D., Macalady, A.K., Griffin, D., Woodhouse, C.A. & Meko, D.M. *et al.* (2013).
846 Temperature as a potent driver of regional forest drought stress and tree mortality. *Nature Climate Change*,
847 3, 292–297.

848 125.

849 Young, D.J.N., Werner, C.M., Welch, K.R., Young, T.P., Safford, H.D. & Latimer, A.M. (2019). Post-fire
850 forest regeneration shows limited climate tracking and potential for drought-induced type conversion. *Ecology*,
851 100, e02571.

852 126.

853 Zhu, Z., Key, C., Ohlen, D. & Benson, N. (2006). *Evaluate sensitivities of burn-severity mapping algorithms*

for different ecosystems and fire histories in the United States (Final Report to the Joint Fire Science Program No. JFSP 01-1-4-12).